0.1 Heteroepitaxy

0.1.1 Pseudomorphic Growth

Comment: *Der folgende Absatz ist probably zu lang, dafür dass ich gar kein pseudomorphic growth beobachte, oder? Aber ich wollte gerne ausrechnen, was denn der out of plane strain* wäre, *falls es so sein sollte, damit ich später argumentieren kann, ob ich relaxed oder pseudomorphic beobachte; oder was dazwischen. Dementsprechend hab ich mich dann gezwungen gefühlt, das ganze noch mal aufzurollen. Vielleicht wäre eine Lösung, (2), (3), (4) und (5) in eine Art appendix zu tun?*

When a body is deformed ("strained") from its original state of equilibrium ("bulk"), forces will arise that tend to return the body to this equilibrium. Molecular forces are the driving element behind these so-called stresses [1]. In continuum mechanics, stress σ_{ij} and strain ϵ_{kl} are symmetric rank-2 tensors that are linearly connected by the elasticity tensor with components C_{ijkl}:

$$\sigma_{ij} = C_{ijkl}\epsilon_{kl}\,, \tag{1}$$

which represents a set of linear equations[1].

If the in-plane (*ip*) lattice constants of two isomorphic compounds match at the interface of a heterostructure, one refers to "pseudomorphic" growth. This case confines some equations of (1):

1. The magnitude of *ip* strain of the thin film material has to be exactly such that the thin film *ip* lattice constants match the substrate *ip* lattice constants.

2. On the other hand, due to vertical growth, the out-of-plane (*oop*) stress of the thin film is demanded to be zero.

The resulting *oop* strain as well as non-diagonal elements of the elasticity tensor can be derived by solving the system of equations (1) with these two boundary conditions. In Grundmann (2018), formulas are derived for the unknown strains in the special case of pseudomorphic heterostructures with threefold rhombohedral symmetry [2]. For numerical predictions of those strains, the elasticity tensor C_{ijkl} of the thin film compound has to be known. But depending on the symmetry of the crystal structure, its components collapse into a lower number of independent entries[2]. For rhombohedral crystals, six independent components are left [3]. An example of the entries of the elasticity tensor for two sesquioxides is given in Tab. 1.

Because of its direct influence on the *oop* lattice plane distance and thus on the X-ray diffraction (XRD) patterns (cf. *tbd*), the strain component perpendicular to the sample surface, ϵ_{zz}, is of particular interest. In the following, the relevant formulas are stated as derived in Ref. [2]. They depend on the respective *ip* strains ϵ_{xx} and ϵ_{yy}

[1] Summation over same indices ("Einstein notation").

[2] Due to symmetry reasons [3], the nine indices ij of the strain tensor can be unambiguously expressed by one index with six possible values: $11 \to 1$, $22 \to 2$, $33 \to 3$, $23 \to 4$, $13 \to 5$, $12 \to 6$ [2]. This allows for a 6×6-matrix representation of the elasticity tensor $C_{ijkl} \to C_{\mu\nu}$.

Table 1: The six independent entries of the elasticity tensor for rhombohedral Cr_2O_3 [4] and α-Ga_2O_3 [2]. All values are in units of 100 GPa.

Material	C_{11}	C_{12}	C_{13}	C_{33}	C_{44}	C_{14}
α-Cr_2O_3	3.74	1.48	1.75	3.62	1.59	−0.19
α-Ga_2O_3	3.82	1.74	1.26	3.46	0.78	−0.17

caused by the lattice mismatch between film and substrate. Note that here, $\mathbf{r} = (x, y, z)$ describes coordinates in the laboratory system – in contrary to Grundmann [2], where $\mathbf{r}$ and $\mathbf{r}'$ are used to describe cartesian coordinates in the crystal and laboratory system, respectively.

One derives for (11.0)-plane (a-orientation):

$$\epsilon_{zz,a} = -\frac{C_{13}\epsilon_{xx,a} + C_{12}\epsilon_{yy,a}}{C_{11}}\,, \tag{2}$$

for (10.0)-plane (m-orientation):

$$\epsilon_{zz,m} = -\frac{C_{13}C_{44}\epsilon_{xx,m} + (C_{12}C_{44} + C_{14}^2)\epsilon_{yy,m}}{C_{11}C_{44} - C_{14}^2}\,, \tag{3}$$

and for (00.1)-plane (c-orientation)

$$\epsilon_{zz,c} = -\frac{2C_{13}}{C_{33}}\epsilon_{yy,c}\,, \tag{4}$$

with $\epsilon_{xx,a} = c_S/c_F - 1$ and $\epsilon_{yy,a} = a_S/a_F - 1$, depending on the lattice parameters of substrate (a_S, c_S) and film (a_F, c_F). Note that $\epsilon_{xx,a} = \epsilon_{xx,m}$, $\epsilon_{yy,a} = \epsilon_{yy,m}$, and $\epsilon_{yy,c} = \epsilon_{yy,a}$. For (01.2)-plane ($r$-orientation), the formula gets more complicated and reads [5]:

$$\epsilon_{zz,r} = \frac{\tau_{zzxx}\epsilon_{xx} + \tau_{zzyy}\epsilon_{yy}}{\mu} \tag{5}$$

$$\ldots\epsilon_{xx} = \textit{tbd} \tag{6}$$

$$\ldots\epsilon_{yy} = \tag{7}$$

$$\ldots\tau_{zzxx} = \zeta_{zzxx} - 2C_{14}(C_{33} + C_{13})\sin 4\theta + 2C_{14}^2\sin^2 2\theta \tag{8}$$

$$\ldots\tau_{zzxx} = \tag{9}$$

$$\ldots\mu = \tag{10}$$

$$\ldots\eta = \ . \tag{11}$$

The distance of lattice planes d orthogonal to the sample surface are then strained, such that:

$$d_{\text{strained}} = d(1 + \epsilon_{zz})\,. \tag{12}$$

Assuming pseudomorphic growth of Cr_2O_3 on Al_2O_3, one can compare the strained lattice plance distances to the unstrained bulk values, by utilizing (12). The numerical values, calculated from the lattice constants (Tab. *tbd*) and the elasticity tensor (Tab. 1), are listed in Tab. 2

Table 2: Comparison of *oop* lattice plane distances for bulk Cr_2O_3 and pseudomorphic Cr_2O_3 on Al_2O_3.

orientation	d	d_{strained}	ϵ_{zz}
c (00.1)	*tbd*		
a (11.0)			
m (10.0)			
r (01.2)			

0.1.2 Relaxed Growth

Dislocations

When the lattice mismatch is not resolved by adaption to the substrate (cf. 0.1.1), the periodicity of the film must be disrupted via so-called dislocations to facilitate relaxed growth of the film. [6]. The highest disturbance from equilibrium spacing happens close to the so-called dislocation line which draws through the material – far away from this line, the crystallinity is restored. In which fashion the distortion happens, can be characterized by the BURGER's vector **b**. The relation of the BURGER's vector to the dislocation line determines the type of the dislocation: if they are orthogonal, one refers to an *edge* dislocation; if they are parallel, one refers to a *screw* dislocation. For a so-called "perfect" dislocation[3], the BURGER's vector is a lattice translation vector. Note that in general, dislocations exhibit both edge- and screw-character [8].

Dislocations are not static, but can move ("glide") inside the crystal. The movement happens typically inside a plane which has highest density of atoms ("glide plane") and along the BURGER's vector which is responsible for the dislocation [8]. The arrangement of glide plane and direction of movement is called "slip system", e.g. for hexagonal structures, one finds $\{00.1\}/\langle 11.0\rangle$ to be one prevailing slip system [8].

For heterostructures with certain slip systems, the relaxation results in an additional tilt of the deposited film. This happens because a BURGER's vector **b** has more than one component: the edge component $b_\parallel$ causes strain relaxation along $b_\parallel$; but if **b** also exhibits a component $b_\perp$ orthogonal to the sample surface and the dislocation line, a tilt angle θ_T will result between substrate and relaxed film:

$$\theta_{T,i} = \epsilon_{ii} \frac{b_{i,\perp}}{b_{i,\parallel}} , \tag{13}$$

where i denotes the axis of strain relaxation. This is schematically depicted in Fig. 1. It's also clear that the dislocation spacing D decreases the tilt *tbd*.

Slip Systems for Sesquioxide Heterostructures

For heteroepitaxial $(Al_xGa_{1-x})_2O_3$-Al_2O_3 systems with low Al content, studies have been conducted on the prevailing relaxation mechanisms for r-oriented [9, 10], as well as a- and m-oriented [6] growth directions. In the following, those results will be

[3] Also referred to as "full" dislocation [7].

summarized. Note that the x-axis points along the c-axis for m- and a-oriented heterostructures, and similarly along the projection of the c-axis on the sample surface for r-oriented heterostructures.

(01.2)-plane (r-orientation) The two relevant slip systems are $\{00.1\}/\frac{1}{3}\langle 11.0\rangle$ and $\{11.0\}/\frac{1}{3}\langle 1\bar{1}.1\rangle$, which contain the "basal" and "prismatic" glide plane, respectively [9]. The former allows for relaxation along the direction containing the projection of the c-axis (x-axis), whereas the latter allows for relaxation perpendicular to it (y-axis). With $\zeta_F = c_F/a_F$, one can determine two possible independent BURGER's vectors $\mathbf{b}_c$ with differing screw components but otherwise same tilt and edge components $b_{c,\perp}$ and $b_{c,\parallel}$, respectively. The tilt along x-direction can then be calculated via:

$$\theta_{T,x} = \epsilon_{xx}\frac{b_{c,\perp}}{b_{c,\parallel}} = \frac{1}{\sqrt{3}}\zeta_F\epsilon_{xx}\,. \tag{14}$$

For the prismatic slip system, the possible BURGER's vectors facilitate relaxation along the y-direction via $b_{a,\parallel}$. But in contrast to the basal system, the tilt components $b_{a,\perp}$ cancel out on average, thus resulting in no net tilt along the y-direction: $\theta_{T,y} = 0$.

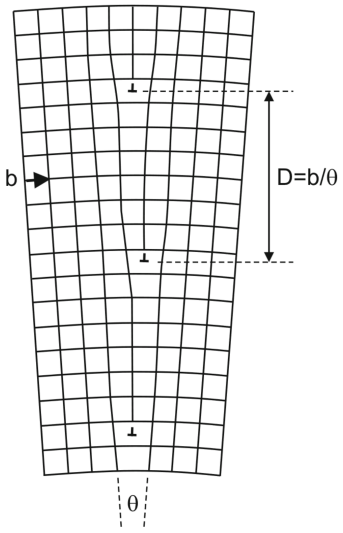

Figure 1: Edge dislocation with BURGER's vector perpendicular to sample surface *tbd*, taken from grundmann2016 *tbd*

(10.0)-plane (m-orientation) Neither basal (00.1) nor prismatic (11.0) and (10.0) slip systems can resolve strain along the x'-axis: The (00.1)-plane is perpendicular to the surface and x-direction, thus the BURGER's vector can only have components in the y-z-plane. But for strain release along x, the BURGER's vector should have some component in this direction, which cannot be the case. The prismatic planes, on the other hand, are perpendicular to the surface but parallel to the x-axis. This results in a dislocation line along the x-direction. To release strain, the BURGER's vector would have x-component, which does not apply for edge dislocations. So the prevailing slip system must have (01.2)-plane (r-orientation) or (11.2)-plane (s-orientation) character, which are called "pyramidal" slip systems. Three different r-planes contribute to strain release, because there is dislocation line component along the y-axis and BURGER's vector's components along the x-axis. With (13) and plugging in the possible BURGER's vectors one finds:

$$\theta_{T,x} = \frac{2}{3}\frac{\sqrt{3}}{\frac{20\zeta}{24+6\zeta^2}+\zeta}\left(\frac{c_S}{c_F}-1\right) \tag{15}$$

(11.0)-plane (a-orientation) The same argument as for the m-oriented heterostructure holds, why only pyramidal slip systems are possible. But in this case, only two r-planes contribute to strain relaxation, because the third plane is perpendicular to the surface, thus can only exhibit BURGER's vectors without in-plane components which results in no possible edge dislocations. Furhtermore, in this case, the BURGER's

Table 3: lorem ipsum lorem ipsum lorem ipsumlorem ipsum lorem ipsum *tbd*

Orientation	$\theta_{T,x'}$	$\theta_{T,y'}$
(01.2) r	yes	no
(11.0) a	no	no
(10.0) m	yes	no

vectors of the two remaining r-planes have opposite tilt components, i.e. they point outwards and inwards of the surface, respectively. Regarding (13), this will result in no net tilt of the thin film.

Bibliography

[1] L. D. Landau and E. M. Lifshitz. *Theory of Elasticity*. Course of Theoretical Physics vol. 7. Pergamon Press Ltd., 1970. 165 pp. ISBN: 978-0-08-057069-3.

[2] Marius Grundmann. "Elastic theory of pseudomorphic monoclinic and rhombohedral heterostructures". In: *Journal of Applied Physics* 124.18 (2018), p. 185302. ISSN: 0021-8979, 1089-7550. DOI: 10.1063/1.5045845.

[3] Neil W. Ashcroft and N. David Mermin. *Solid State Physics*. Saunders College Publishing, 1976. 826 pp.

[4] H.L. Alberts and J.C.A. Boeyens. "The elastic constants and distance dependence of the magnetic interactions of Cr_2O_3". In: *Journal of Magnetism and Magnetic Materials* 2.4 (1976), pp. 327–333. ISSN: 03048853. DOI: 10.1016/0304-8853(76)90044-5.

[5] Marius Grundmann. "A most general and facile recipe for the calculation of heteroepitaxial strain". In: *physica status solidi (b)* 257.12 (2020), p. 2000323. ISSN: 0370-1972, 1521-3951. DOI: 10.1002/pssb.202000323.

[6] Max Kneiß et al. "Strain states and relaxation for α-$(Al_xGa_{1-x})_2O_3$ thin films on prismatic planes of α-Al_2O_3 in the full composition range: Fundamental difference of a- and m-epitaxial planes in the manifestation of shear strain and lattice tilt". In: *Journal of Materials Research* 36.23 (2021), pp. 4816–4831. ISSN: 0884-2914, 2044-5326. DOI: 10.1557/s43578-021-00375-3.

[7] Marius Grundmann. *The Physics of Semiconductors: An Introduction Including Nanophysics and Applications*. Graduate Texts in Physics. Cham: Springer International Publishing, 2016. ISBN: 978-3-319-23879-1 978-3-319-23880-7. URL: http://link.springer.com/10.1007/978-3-319-23880-7.

[8] Derek Hull and D. J. Bacon. *Introduction to Dislocations*. 5th ed. Elsevier Ltd., 2011. 268 pp. ISBN: 978-0-08-096673-1.

[9] M. Grundmann and M. Lorenz. "Anisotropic strain relaxation through prismatic and basal slip in α-(Al, Ga)$_2O_3$ on R-plane Al_2O_3". In: *APL Materials* 8.2 (2020), p. 021108. ISSN: 2166-532X. DOI: 10.1063/1.5144744.

[10] M. Grundmann, T. Stralka, and M. Lorenz. "Epitaxial growth and strain relaxation of corundum-phase $(Al,Ga)_2O_3$ thin films from pulsed laser deposition at 1000 °C on r-plane Al_2O_3". In: *Applied Physics Letters* 117.24 (2020), p. 242102. ISSN: 0003-6951, 1077-3118. DOI: 10.1063/5.0030675.